Measurement of Day and Night Neutrino Energy Spectra at SNO and Constraints on Neutrino Mixing Parameters

Q.R. Ahmad,[17] R.C. Allen,[4] T.C. Andersen,[6] J.D. Anglin,[10] J.C. Barton,[11,*] E.W. Beier,[12] M. Bercovitch,[10] J. Bigu,[7] S.D. Biller,[11] R.A. Black,[11] I. Blevis,[5] R.J. Boardman,[11] J. Boger,[3] E. Bonvin,[14] M.G. Boulay,[9,14] M.G. Bowler,[11] T.J. Bowles,[9] S.J. Brice,[9,11] M.C. Browne,[17,9] T.V. Bullard,[17] G. Bühler,[4] J. Cameron,[11] Y.D. Chan,[8] H.H. Chen,[4,†] M. Chen,[14] X. Chen,[8,11] B.T. Cleveland,[11] E.T.H. Clifford,[14] J.H.M. Cowan,[7] D.F. Cowen,[12] G.A. Cox,[17] X. Dai,[11] F. Dalnoki-Veress,[5] W.F. Davidson,[10] P.J. Doe,[17,9,4] G. Doucas,[11] M.R. Dragowsky,[9,8] C.A. Duba,[17] F.A. Duncan,[14] M. Dunford,[12] J.A. Dunmore,[11] E.D. Earle,[14,1] S.R. Elliott,[17,9] H.C. Evans,[14] G.T. Ewan,[14] J. Farine,[7,5] H. Fergani,[11] A.P. Ferraris,[11] R.J. Ford,[14] J.A. Formaggio,[17] M.M. Fowler,[9] K. Frame,[11] E.D. Frank,[12] W. Frati,[12] N. Gagnon,[11,9,8,17] J.V. Germani,[17] S. Gil,[2] K. Graham,[14] D.R. Grant,[5] R.L. Hahn,[3] A.L. Hallin,[14] E.D. Hallman,[7] A.S. Hamer,[9,14] A.A. Hamian,[17] W.B. Handler,[14] R.U. Haq,[7] C.K. Hargrove,[5] P.J. Harvey,[14] R. Hazama,[17] K.M. Heeger,[17] W.J. Heintzelman,[12] J. Heise,[2,9] R.L. Helmer,[16,2] J.D. Hepburn,[14] H. Heron,[11] J. Hewett,[7] A. Hime,[9] J.G. Hykawy,[7] M.C.P. Isaac,[8] P. Jagam,[6] N.A. Jelley,[11] C. Jillings,[14] G. Jonkmans,[7,1] K. Kazkaz,[17] P.T. Keener,[12] J.R. Klein,[12] A.B. Knox,[11] R.J. Komar,[2] R. Kouzes,[13] T. Kutter,[2] C.C.M. Kyba,[12] J. Law,[6] I.T. Lawson,[6] M. Lay,[11] H.W. Lee,[14] K.T. Lesko,[8] J.R. Leslie,[14] I. Levine,[5] W. Locke,[11] S. Luoma,[7] J. Lyon,[11] S. Majerus,[11] H.B. Mak,[14] J. Maneira,[14] J. Manor,[17] A.D. Marino,[8] N. McCauley,[12,11] D.S. McDonald,[12] A.B. McDonald,[14,13] K. McFarlane,[5] G. McGregor,[11] R. Meijer Drees,[17] C. Mifflin,[5] G.G. Miller,[9] G. Milton,[1] B.A. Moffat,[14] M. Moorhead,[11] C.W. Nally,[2] M.S. Neubauer,[12] F.M. Newcomer,[12] H.S. Ng,[2] A.J. Noble,[16,5] E.B. Norman,[8] V.M. Novikov,[5] M. O'Neill,[5] C.E. Okada,[8] R.W. Ollerhead,[6] M. Omori,[11] J.L. Orrell,[17] S.M. Oser,[12] A.W.P. Poon,[8,17,2,9] T.J. Radcliffe,[14] A. Roberge,[7] B.C. Robertson,[14] R.G.H. Robertson,[17,9] S.S.E. Rosendahl,[8] J.K. Rowley,[3] V.L. Rusu,[12] E. Saettler,[7] K.K. Schaffer,[17] M.H. Schwendener,[7] A. Schülke,[8] H. Seifert,[7,17,9] M. Shatkay,[5] J.J. Simpson,[6] C.J. Sims,[11] D. Sinclair,[5] P. Skensved,[14] A.R. Smith,[8] M.W.E. Smith,[17] T. Spreitzer,[12] N. Starinsky,[5] T.D. Steiger,[17] R.G. Stokstad,[8] L.C. Stonehill,[17] R.S. Storey,[10,†] B. Sur,[1,14] R. Tafirout,[7] N. Tagg,[6,11] N.W. Tanner,[11] R.K. Taplin,[11] M. Thorman,[11] P.M. Thornewell,[11] P.T. Trent,[11] Y.I. Tserkovnyak,[2] R. Van Berg,[12] R.G. Van de Water,[9,12] C.J. Virtue,[7] C.E. Waltham,[2] J.-X. Wang,[6] D.L. Wark,[15,11,9] N. West,[11] J.B. Wilhelmy,[9] J.F. Wilkerson,[17,9] J.R. Wilson,[11] P. Wittich,[12] J.M. Wouters,[9] and M. Yeh[3]

(SNO Collaboration)

[1] *Atomic Energy of Canada, Limited, Chalk River Laboratories, Chalk River, ON K0J 1J0, Canada*
[2] *Department of Physics and Astronomy, University of British Columbia, Vancouver, BC V6T 1Z1 Canada*
[3] *Chemistry Department, Brookhaven National Laboratory, Upton, NY 11973-5000*
[4] *Department of Physics, University of California, Irvine, CA 92717*
[5] *Carleton University, Ottawa, Ontario K1S 5B6 Canada*
[6] *Physics Department, University of Guelph, Guelph, Ontario N1G 2W1 Canada*
[7] *Department of Physics and Astronomy, Laurentian University, Sudbury, Ontario P3E 2C6 Canada*
[8] *Institute for Nuclear and Particle Astrophysics and Nuclear Science Division, Lawrence Berkeley National Laboratory, Berkeley, CA 94720*
[9] *Los Alamos National Laboratory, Los Alamos, NM 87545*
[10] *National Research Council of Canada, Ottawa, ON K1A 0R6, Canada*
[11] *Department of Physics, University of Oxford, Denys Wilkinson Building, Keble Road, Oxford, OX1 3RH, UK*
[12] *Department of Physics and Astronomy, University of Pennsylvania, Philadelphia, PA 19104-6396*
[13] *Department of Physics, Princeton University, Princeton, NJ 08544*
[14] *Department of Physics, Queen's University, Kingston, Ontario K7L 3N6 Canada*
[15] *Rutherford Appleton Laboratory, Chilton, Didcot, Oxon, OX11 0QX, and University of Sussex, Physics and Astronomy Department, Brighton BN1 9QH, UK*
[16] *TRIUMF, 4004 Wesbrook Mall, Vancouver, BC V6T 2A3, Canada*
[17] *Center for Experimental Nuclear Physics and Astrophysics, and Department of Physics, University of Washington, Seattle, WA 98195*

(Dated: April 19, 2002)

The Sudbury Neutrino Observatory (SNO) has measured day and night solar neutrino energy spectra and rates. For charged current events, assuming an undistorted ^{8}B spectrum, the night minus day rate is $14.0\% \pm 6.3\%^{+1.5}_{-1.4}\%$ of the average rate. If the total flux of active neutrinos is additionally constrained to have no asymmetry, the ν_e asymmetry is found to be $7.0\% \pm 4.9\%^{+1.3}_{-1.2}\%$. A global solar neutrino analysis in terms of matter-enhanced oscillations of two active flavors strongly favors the Large Mixing Angle (LMA) solution.

PACS numbers: 26.65.+t, 14.60.Pq, 13.15.+g, 95.85.Ry

The Sudbury Neutrino Observatory (SNO) has provided strong evidence that neutrinos change flavor as they propagate from the core of the Sun [1, 2], independently of solar model flux predictions. This flavor conversion can be explained by neutrino oscillation models based on flavor mixing. For some values of the mixing parameters, spectral distortions and a measurable dependence on solar zenith angle are expected [3–5]. The latter might be caused by interaction with the matter of the Earth (the MSW effect) and would depend not only on oscillation parameters and neutrino energy, but also on the path length and e^- density through the Earth. This Letter presents SNO's first measurements of day and night neutrino energy spectra, and constraints on allowed neutrino mixing parameters.

The data reported here were recorded between November 2, 1999 and May 28, 2001 UTC. The total livetimes for day and night are 128.5 and 177.9 days, respectively. The time-averaged inverse-square distance to the Sun $\langle(\frac{1AU}{R})^2\rangle$ was 1.0002 (day) and 1.0117 (night). During the development of this analysis, the data were partitioned into two sets of approximately equal livetime (split at July 1, 2000), each having substantial day and night components. Analysis procedures were refined during the analysis of Set 1 and fixed before Set 2 was analysed. The latter thus served as an unbiased test. Unless otherwise stated, the analysis presented in this paper is for the combined data set.

The data reduction in [1] was used here. For each event, the number, pattern, and timing of the hit photomultiplier tubes (PMTs) were used to reconstruct effective recoil electron kinetic energy T_{eff}, radial position R, and scattering angle $\theta_\odot$ with respect to the Sun-Earth direction. The charged current (CC), elastic scattering (ES) and neutral current (NC) reactions each have characteristic probability density functions (pdfs) of T_{eff}, R, and $\theta_\odot$. A maximum likelihood fit of the pdfs to the data determined the flux from each of these reactions.

The measured night and day fluxes ϕ_N and ϕ_D were used to form the asymmetry ratio for each reaction: $\mathcal{A} = 2(\phi_N - \phi_D)/(\phi_N + \phi_D)$. The CC interaction is sensitive only to ν_e. The NC interaction is equally sensitive to all active neutrino flavors, so active-only neutrino models predict $\mathcal{A}_{NC} = 0$ [6]. The same models allow $\mathcal{A}_{CC} \neq 0$. The ES reaction has additional contributions from $\nu_{\mu\tau}$ leading to a reduction in its sensitivity to ν_e asymmetries.

SNO used calibration sources [7] to constrain variations in detector response [8] that can lead to day-night asymmetries. A ^{16}N source [9], which produces 6.1-MeV gamma rays, revealed a 1.3% per year drift in the energy scale. Due to seasonal variation in day and night livetime, this drift can create an artificial asymmetry. The analysis corrected for this drift and a systematic uncertainty was assigned using worst-case drift models. Gamma rays from the ^{16}N source were also used to constrain directional dependences in SNO's response.

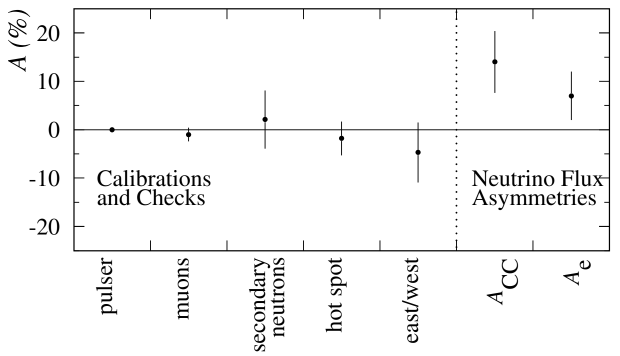

FIG. 1: Various event classes used to determine systematic differences between day and night measurements. Also shown are measured asymmetries on the CC flux, and on the electron neutrino flux derived from the CC, ES, and NC rates when the total neutrino flux is constrained to have zero asymmetry.

A set of signals that are continuously present in the detector was used to probe possible diurnal variations in detector response. The detector was triggered at 5 Hz with a pulser, verifying livetime accounting. Muons provide an almost constant signal and, through interactions with D_2O, produce secondary neutrons. After applying a cut to remove bursts with high neutron multiplicity, these muon-induced neutrons were used to limit temporal variations in detector response. A more sensitive study focused on a solitary point of high background radioactivity, or "hot spot", on the upper hemisphere of the SNO acrylic vessel, apparently introduced during construction. Its event rate was stable and sufficient to make an excellent test of diurnal variations. It also provides a sensitive test for changes in reconstruction. A limit of 3.5% on the hot spot rate asymmetry was determined, which because of its steeply falling energy spectrum constrained the day and night energy scales to be the same within 0.3%. An east/west division of the neutrino data based on the Sun's position should show no rate variations from matter effects. As expected, the CC rates for east and west data were consistent. The rate asymmetries for each test are shown in Fig. 1.

Backgrounds were subtracted separately for day and night as part of the signal extraction. The results were normalized for an Earth-Sun distance of 1 AU, yielding the results in Table I. Day and night fluxes are given separately for data Sets 1 and 2, and for the combined data. A χ^2 consistency test of the six measured fluxes

*Permanent Address: Birkbeck College, University of London, Malet Road, London WC1E 7HX, UK
†Deceased

TABLE I: The results of signal extraction, assuming an undistorted ^{8}B spectrum. The systematic uncertainties (combined set) include a component that cancels in the formation of the $\mathcal{A}$. Except for the dimensionless $\mathcal{A}$, the units are 10^6 cm^{-2} s^{-1}.

	Set 1		Set 2		Combined		$\mathcal{A}$(%)
signal	ϕ_D	ϕ_N	ϕ_D	ϕ_N	ϕ_D	ϕ_N	
CC	1.53 ± 0.12	1.95 ± 0.10	1.69 ± 0.12	1.77 ± 0.11	$1.62 \pm 0.08 \pm 0.08$	$1.87 \pm 0.07 \pm 0.10$	$+14.0 \pm\ 6.3^{+1.5}_{-1.4}$
ES	2.91 ± 0.52	1.59 ± 0.38	2.35 ± 0.51	2.88 ± 0.47	$2.64 \pm 0.37 \pm 0.12$	$2.22 \pm 0.30 \pm 0.12$	$-17.4 \pm 19.5^{+2.4}_{-2.2}$
NC	7.09 ± 0.97	3.95 ± 0.75	4.56 ± 0.89	5.33 ± 0.84	$5.69 \pm 0.66 \pm 0.44$	$4.63 \pm 0.57 \pm 0.44$	$-20.4 \pm 16.9^{+2.4}_{-2.5}$

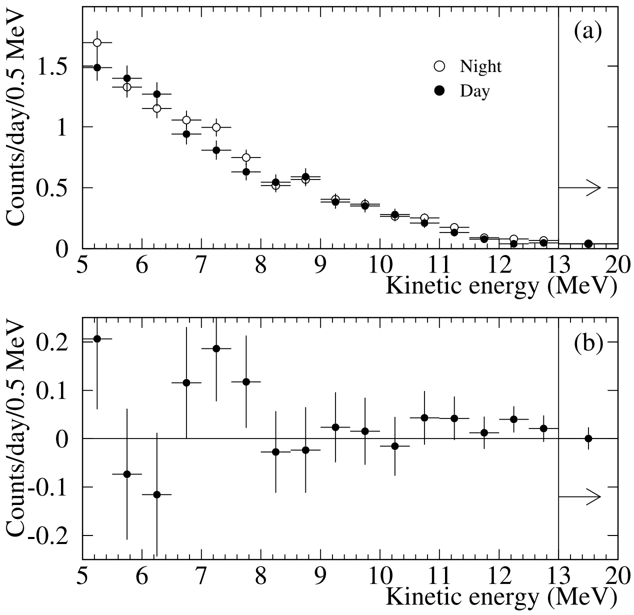

FIG. 2: (a) Energy spectra for day and night. All signals and backgrounds contribute. The final bin extends from 13.0 to 20.0 MeV. (b) Difference, *night - day*, between the spectra. The day rate was 9.23 ± 0.27 events/day, and the night rate was 9.79 ± 0.24 events/day.

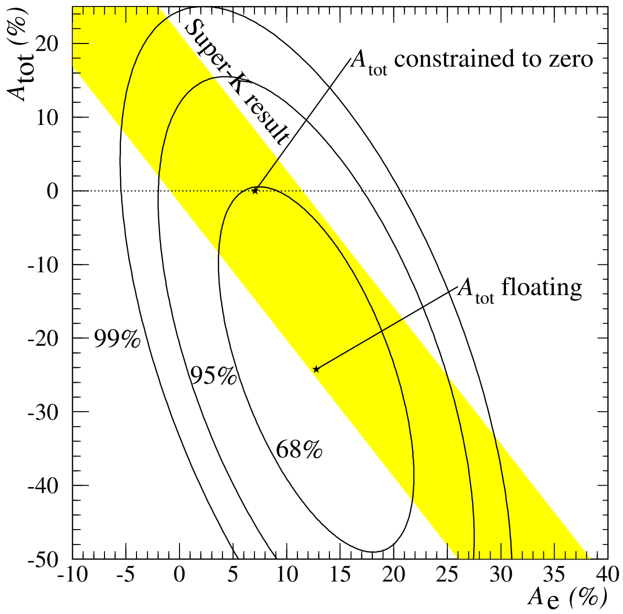

FIG. 3: Joint probability contours for $\mathcal{A}_{tot}$ and $\mathcal{A}_e$. The points indicate the results when $\mathcal{A}_{tot}$ is allowed to float and when it is constrained to zero. The diagonal band indicates the 68% joint contour for the Super-K $\mathcal{A}_{ES}$ measurement.

between Sets 1 and 2 yielded a chance probability of 8%. A similar test done directly on the three asymmetry parameters gave a chance probability of 2%. No systematic has been identified, in either signal or background regions, that would suggest that the differences between Set 1 and Set 2 are other than a statistical fluctuation. For the combined analysis, $\mathcal{A}_{CC}$ is $+2.2\sigma$ from zero, while $\mathcal{A}_{ES}$ and $\mathcal{A}_{NC}$ are -0.9σ and -1.2σ from zero, respectively. Note that $\mathcal{A}_{CC}$ and $\mathcal{A}_{NC}$ are strongly statistically anti-correlated ($\rho = -0.518$), while $\mathcal{A}_{CC}$ and $\mathcal{A}_{ES}$ ($\rho = -0.161$) and $\mathcal{A}_{ES}$ and $\mathcal{A}_{NC}$ ($\rho = -0.106$) are moderately anti-correlated. Table II gives the systematic uncertainties on the asymmetry parameters. The day and night energy spectra for all accepted events are shown in Fig. 2.

Table III (a) shows the results for $\mathcal{A}_e$ derived from the CC day and night rate measurements, i.e., $\mathcal{A}_e = \mathcal{A}_{CC}$. The day and night flavor contents were then extracted by changing variables to $\phi_{CC} = \phi_e$, $\phi_{NC} = \phi_{tot} = \phi_e + \phi_{\mu\tau}$ and $\phi_{ES} = \phi_e + \epsilon\phi_{\mu\tau}$, where $\epsilon \equiv 1/6.48$ is the ratio of the average ES cross sections above 5 MeV for $\nu_{\mu\tau}$ and ν_e. Table III (b) shows the asymmetries of ϕ_e and ϕ_{tot} with this additional constraint from the ES rate measurements. This analysis allowed for an asymmetry in the total flux of ^{8}B neutrinos (non-zero $\mathcal{A}_{tot}$), with the measurements of $\mathcal{A}_e$ and $\mathcal{A}_{tot}$ having a strong anti-correlation. Fig. 3 shows the $\mathcal{A}_e$ vs. $\mathcal{A}_{tot}$ joint probability contours. Forcing $\mathcal{A}_{tot} = 0$, as predicted by active-only models, yielded the result in Table III (c) of $\mathcal{A}_e = 7.0\% \pm 4.9\%$ (stat.)$^{+1.3}_{-1.2}$% (sys.).

The Super-Kamiokande (SK) collaboration measured $\mathcal{A}_{ES}(SK) = 3.3\% \pm 2.2\%$ (stat.)$^{+1.3}_{-1.2}$% (sys.) [10]. The ES measurement includes a neutral current component, which reduces the asymmetry for this reaction relative to $\mathcal{A}_e$ [11]. $\mathcal{A}_{ES}(SK)$ may be converted to an equivalent electron flavor asymmetry using the total neutrino flux measured by SNO, yielding $\mathcal{A}_e(SK)$ (Table III (d)). This value is in good agreement with SNO's direct measure-

TABLE II: Effect of systematic uncertainties on $\mathcal{A}$ (%). For presentation, uncertainties have been symmetrized and rounded.

Systematic	$\delta\mathcal{A}_{CC}$	$\delta\mathcal{A}_{ES}$	$\delta\mathcal{A}_{NC}$
Long-term energy scale drift	0.4	0.5	0.2
Diurnal energy scale variation	1.2	0.7	1.6
Directional energy scale var.	0.2	1.4	0.3
Diurnal energy resolution var.	0.1	0.1	0.3
Directional energy resolution var.	0.0	0.1	0.0
Diurnal vertex shift var.	0.5	0.6	0.7
Directional vertex shift var.	0.0	1.1	0.1
Diurnal vertex resolution var.	0.2	0.7	0.5
Directional angular recon. var.	0.0	0.1	0.1
PMT β-γ background	0.0	0.2	0.5
AV+H_2O β-γ bkgd.	0.0	0.6	0.2
D_2O β-γ, neutrons bkgd.	0.1	0.4	1.2
External neutrons bkgd.	0.0	0.2	0.4
Sacrifice	0.5	0.5	0.5
Total	1.5	2.4	2.4

TABLE III: Measurement of the ϕ_e and ϕ_{tot} asymmetry for various constraints. All analyses assume an undistorted ^{8}B spectrum.

Constraints	Asymmetry (%)
a) no additional constraint	$\mathcal{A}_{CC} = 14.0 \pm 6.3^{+1.5}_{-1.4}$ $\mathcal{A}_{NC} = -20.4 \pm 16.9^{+2.4}_{-2.5}$ (see text for correlations)
b) $\phi_{ES} = (1-\epsilon)\phi_e + \epsilon\phi_{tot}$	$\mathcal{A}_e = 12.8 \pm 6.2^{+1.5}_{-1.4}$ $\mathcal{A}_{tot} = -24.2 \pm 16.1^{+2.4}_{-2.5}$ correlation = -0.602
c) $\phi_{ES} = (1-\epsilon)\phi_e + \epsilon\phi_{tot}$ $\mathcal{A}_{tot} = 0$	$\mathcal{A}_e = 7.0 \pm 4.9^{+1.3}_{-1.2}$
d) $\phi_{ES} = (1-\epsilon)\phi_e + \epsilon\phi_{tot}$ $\mathcal{A}_{tot} = 0$ $\mathcal{A}_{ES}(SK) = 3.3\% \pm 2.2\%^{+1.3}_{-1.2}\%$	$\mathcal{A}_e(SK) = 5.3 \pm 3.7^{+2.0}_{-1.7}$ (derived from SK $\mathcal{A}_{ES}$ and SNO total ^{8}B flux)

ment of $\mathcal{A}_e$, as seen in Fig. 3.

SNO's day and night energy spectra (Fig. 2) have also been used to produce MSW exclusion plots and limits on neutrino flavor mixing parameters. MSW oscillation models between two active flavors were fit to the data. For simplicity, only the energy spectra were used in the fit, and the radial R and direction $\cos\theta_\odot$ information was omitted. This procedure preserves most of the ability to discriminate between oscillation solutions. A model was constructed for the expected number of counts in each energy bin by combining the neutrino spectrum [12], the survival probability, and the cross sections [13] with SNO's response functions [8].

There are 3 free parameters in the fit: the total ^{8}B flux ϕ_B, the difference Δm^2 between the squared masses of the two neutrino mass eigenstates, and the mixing angle θ. The flux of higher energy neutrinos from the solar *hep* reaction was fixed at 9.3×10^3 cm^{-2} s^{-1} [14]. Contours were generated in Δm^2 and $\tan^2\theta$ for $\Delta\chi^2(c.l.) =$ 4.61 (90%), 5.99 (95%), 9.21 (99%), and 11.83 (99.73%). Fig. 4(a) shows allowed mixing parameter regions using only SNO data with no additional experimental constraints or inputs from solar models. By including flux information from the Cl [15] and Ga experiments [16–20], the day and night spectra from the SK experiment [10], along with solar model predictions for the more robust *pp*, *pep* and ^{7}Be neutrino fluxes [14], the contours shown in Fig. 4(b) were produced. This global analysis strongly favors the Large Mixing Angle (LMA) region (see Table IV), and $\tan^2\theta$ values < 1. Repeating the global analysis using the total SNO energy spectrum instead of separate day and night spectra gives nearly identical results.

In summary, SNO has measured the day-night asymmetries of the CC, NC, and ES reaction rates. From these results the first direct measurements of the day-night asymmetries in the ν_e flux and the total ν flux from the Sun have been deduced. A global fit to SNO's day and night energy spectra and data from other solar neutrino experiments strongly favors the LMA solution in a 2-flavor MSW neutrino oscillation analysis.

This research was supported by: Canada: NSERC, Industry Canada, NRC, Northern Ontario Heritage Fund Corporation, Inco, AECL, Ontario Power Generation; US: Dept. of Energy; UK: PPARC. We thank the SNO technical staff for their strong contributions.

TABLE IV: Best fit points in the MSW plane for global MSW analysis using all solar neutrino data. ϕ_B is the best-fit ^{8}B flux for each point, and has units of 10^6 cm^{-2} s^{-1}. Δm^2 has units of eV^2. $\mathcal{A}_e$ is the predicted asymmetry for each point.

Region	χ^2_{min}/dof	ϕ_B	$\mathcal{A}_e$(%)	Δm^2	$\tan^2\theta$	c.l.(%)
LMA	57.0/72	5.86	6.4	5.0×10^{-5}	0.34	—
LOW	67.7/72	4.95	5.9	1.3×10^{-7}	0.55	99.5

[1] Q. R. Ahmad *et al.*, Phys. Rev. Lett. (2002), SNO NC PRL, submitted for publication.
[2] Q. R. Ahmad *et al.*, Phys. Rev. Lett. **87**, 071301 (2001).
[3] S. P. Mikheyev and A. Y. Smirnov, in *'86 Massive Neutrinos in Astrophysics and in Particle Physics, Proceedings of the Moriond Workshop*, edited by O. Fackler and J. Tran Thanh Van (1986), vol. Editions Frontières, Gif-sur-Yvette, 1986, p. 335.
[4] A. J. Baltz and J. Weneser, Phys. Rev. D **37**, 3364 (1988).
[5] M. C. Gonzalez-Garcia, C. Peña-Garay and A. Y. Smirnov, Phys. Rev. D **63**, 113004 (2001).
[6] A non-zero value for $\mathcal{A}_{NC}$ might be evidence for sterile neutrinos.
[7] The SNO Collaboration, Nucl. Instr. and Meth. **A449**, 172 (2000).
[8] Details of SNO response functions are available from the

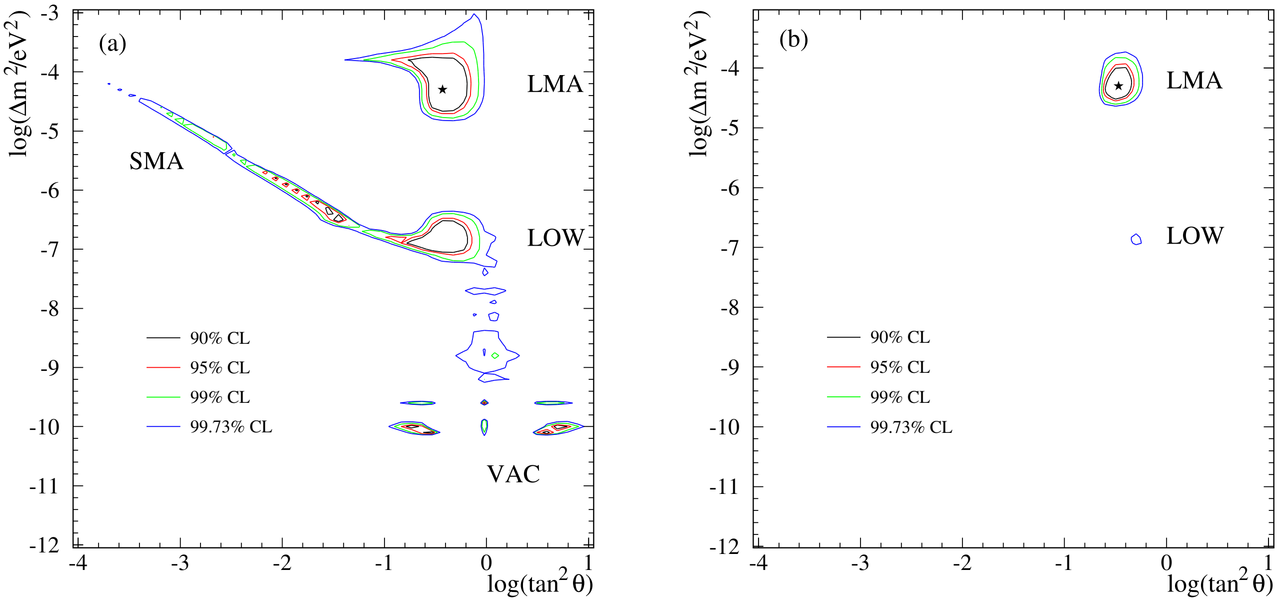

FIG. 4: Allowed regions of the MSW plane determined by a χ^2 fit to (a) SNO day and night energy spectra and (b) with additional experimental and solar model data. The star indicates the best fit. See text for details.

SNO web site: http://sno.phy.queensu.ca
[9] M. Dragowsky *et al.*, Nucl. Instr. and Meth. **A481**, 284 (2002).
[10] S. Fukuda *et al.*, Phys. Rev. Lett. **86**, 5651 (2001).
[11] J. N. Bahcall, M. C. Gonzalez-Garcia, and C. Peña-Garay (2002), hep-ph/0111150 v2.
[12] C. E. Ortiz *et al.*, Phys. Rev. Lett. **85**, 2909 (2000).
[13] S. Nakamura *et al.* (2002), nucl-th/0201062.
[14] J. N. Bahcall, H. M. Pinsonneault and S. Basu, Astrophys. J **555**, 990 (2001).
[15] B. T. Cleveland *et al.*, Astrophys. J **496**, 505 (1998).
[16] J. N. Abdurashitov *et al.*, Phys. Rev. C **60**, 055801 (1999).
[17] J. N. Abdurashitov *et al.* (2002), astro-ph/0204245
[18] M. Altmann *et al.*, Phys. Lett. B **490**, 16 (2000).
[19] W. Hampel *et al.*, Phys. Lett. B **447**, 127 (1999).
[20] C. M. Cattadori *et al.*, in *Proceedings of the TAUP 2001 Workshop*, (September 2001), Assergi, Italy.